Sensitivity of ion-induced sputtering to the radial distribution of energy transfers: A molecular dynamics study

S. Mookerjee,[1,*] M. Beuve,[2,3] S. A. Khan,[1] M. Toulemonde,[4] and A. Roy[1]
[1]*Inter University Accelerator Centre, Aruna Asaf Ali Marg, New Delhi 110067, India*
[2]*Universite de Lyon and Universite Lyon 1, Lyon, F-69003, France*
[3]*Institut de Physique Nucleaire de Lyon (IPNL), IN2P3-CNRS-UMR5822, Villeurbanne, F69622, France*
[4]*CIRIL, Laboratoire commun CEA-CNRS-ENSICAEN-UCBN, Boulevard H. Becquerel, Boite Postale 5133, 14070 Caen Cedex 5, France*
(Received 17 January 2008; revised manuscript received 24 June 2008; published 31 July 2008)

Using different models for the deposition of energy on the lattice and a classical molecular dynamics approach to the subsequent transport, we evaluate how the details of the energy deposition model influence sputtering yield from a Lennard-Jones target irradiated with a MeV/u ion beam. Two energy deposition models are considered: a uniform, instantaneous deposition into a cylinder of fixed radius around the projectile ion track, used in earlier molecular dynamics and fluid dynamics simulations of sputtering yields; and an energy deposition distributed in time and space based on the formalism developed in the thermal spike model. The dependence of the sputtering yield on the total energy deposited on the target atoms is very sensitive to the energy deposition model. To clarify the origin of this strong dependence, we explore the role of the radial expansion of the electronic system prior to the transfer of its energy to the lattice. The results imply that observables such as the sputtering yield may be used as signatures of the fast electron-lattice energy transfer in the electronic energy-loss regime, and indicate the need for more experimental and theoretical investigations of these processes.

DOI: 10.1103/PhysRevB.78.045435 PACS number(s): 61.80.Lj, 79.20.Rf, 79.20.Ap

I. INTRODUCTION

Irradiation of targets by MeV/u ion beams have found many important applications in recent years, ranging from nanomaterials[1–3] to radiation therapy.[4] Improved modeling using Monte Carlo and molecular dynamics techniques, and a wealth of experimental data have led to a detailed understanding of the loss of projectile energy to the electronic system and also of the displacement of lattice atoms on receiving this energy. However, there is less clarity about the mechanisms of transfer of energy from the electronic system to the lattice in this electronic stopping regime.[5,6] This is particularly difficult to study experimentally given the femtosecond time scales for the transfer because experimental observables may be expected to carry signatures of the long relaxation phase.

It is therefore necessary to explore computational models that may relate the energy deposition process and the subsequent atomic transport to experimental observables. Full first-principles calculations of the electron-lattice coupling and energy transfer after ion irradiation are likely to remain computationally prohibitive. Insights may still be gained, however, from models with simplifying assumptions. In particular, the thermal spike model has had some success in explaining results on track formation[7,8] and sputtering,[9–11] assuming a radial expansion of the deposited energy on the electrons prior to its transfer to the lattice. Molecular dynamics starting from an assumed energy deposition on the lattice[12–16] and fluid dynamics[17,18] simulations also provide a way to link observables such as sputtering[15] and amorphization[16] to the electron-lattice energy-transfer process.

To interpret results from these techniques and compare with experiment, it is necessary to understand the effect of the model assumptions on the observables. The systematics of the sputter yield, in particular the dependence of the yield on the deposited energy, are different for the analytical thermal spike model, and the fluid dynamics and molecular dynamics calculations.[9–11,14,18] These differences have been attributed[13,18,19] to the diffusive transport mechanism postulated by the thermal spike model after energy deposition on the lattice. Besides the mass and energy transport mechanisms, the thermal spike, and the molecular and fluid dynamics models also differ in the details of the initial deposition of energy on the lattice from the electronic system. It has been pointed out that the spatial[14,15] and temporal[15] distributions of the deposited energy influence the predicted sputtering yield.

In this work, we use a molecular dynamics simulation of a Lennard-Jones (LJ) solid to explore the influence of the radial distribution of deposited energy on the sputtering yield. Two models that yield different radial deposited energy distributions are studied: a uniform deposition into a cylinder of fixed radius around the projectile track core and a deposition mechanism derived from the thermal spike model. In this latter case, the energy is deposited on the lattice through a heat exchange between the electronic and atomic systems that evolves in time. We note, however, that the transfer process is still extremely fast compared to the atomic displacements leading to sputtering and it is possible to define approximately an initial deposition for comparison with the instantaneous deposition into a fixed-radius cylinder.

The choice of the Lennard-Jones potential enables this work to complement previous studies, including a study[13] of the change of the calculated yield on changing from a diffusive to a molecular dynamics prescription for the postdeposition atomic transport in the target. We show that, for the

same molecular dynamics transport, the yield is sensitive to the radial distribution over a large range of deposited energies. Bringa and co-workers have shown in a series of papers[13,20–22] that the equations of motion and results, using the 12–6 Lennard-Jones potential scale with the cohesive energy U and number density n. They have also shown that the scaling is roughly preserved for more complex potentials.[14] General results from simulations using the Lennard-Jones potential may then, with some caution, be extended to other systems as well. A comparison of the results of our simulation, using a Lennard-Jones target with analytical thermal spike model calculations[23] of Si sputtering from SiO_2, might be expected to isolate the effect of the transport and sputtering mechanisms alone. This comparison is flawed here, however, by the different projectile velocities used in the present work and in Ref. 23, as also by the different electron-phonon coupling. As a result, the radial distribution of energy deposited on the lattice is quite different in the two cases. Nonetheless, it is possible to notice that the threshold electronic energy loss for the onset of sputtering is similar; the relationship between yield and electronic energy loss is, on the other hand, significantly different.

The sputtering yield is also then useful as an observable signal to the details of the femtosecond electron-lattice energy-transfer process; however, this sensitivity implies the need to model the electron-lattice energy-transfer process accurately for a meaningful comparison of molecular dynamics simulations with experimental sputtering yields.

II. DETAILS OF CALCULATIONS

The calculation uses the IMPACT molecular dynamics code,[12,15] a linked-cell velocity Verlet molecular dynamics program for sputtering from an irradiated target with a provision for incorporating additional energy transfers to the lattice atoms during the course of the simulation. The calculations are carried out in two modes: a standard calculation in which all energy is dumped on to atoms in a predefined cylinder around the projectile track and a calculation in which the lattice atoms receive energy continuously from a hot-electron gas. We henceforth refer to these two modes as cylindrical and thermal spike depositions, respectively. The potential used is a standard Lennard-Jones potential with parameters adjusted[12–15] to correspond to Ar. We emphasize that we use this only as a model system to explore the effect of the radial distribution of deposited energy on sputtering yields. In particular, as pointed out in Ref. 15, we do not model excitons. We also choose values of the electron-phonon coupling to emphasize the effect of the radial distribution of deposited energy on sputtering and not for any relationship with the actual values of Ar. For both cylindrical and thermal spike depositions, the velocity of the incident ion is constrained to be that corresponding to a 1 MeV H ion for all values of the electronic energy loss considered here. All surfaces are treated as free surfaces. Sample sizes range from $90\times90\times50$ monolayers for cylindrical and thermal spike depositions at low electronic energy loss to $126\times126\times60$ monolayers for thermal spike deposition at large electronic loss values. The sizes have been determined to be large enough that the free side surfaces have no impact on the results presented here.

The spatial and temporal distributions of the energy deposited on the atoms in the target, due to the electronic energy loss S_e, depends on whether the deposition is cylindrical or thermal, and on the parameters of the thermal spike deposition model. For cylindrical deposition, all atoms in a cylinder of fixed radius are assumed to equally and instantaneously share the entire electronic energy loss; in our calculations, the S_e for cylindrical deposition is distributed equally to all atoms in a 7 Å cylinder at the beginning of the simulation. For the thermal spike deposition, it is the electronic subsystem that is assumed to gain the entire S_e at the beginning of the simulation. Subsequently, the electron gas expands radially through electronic cascades and cools down, transferring energy to the lattice until thermal equilibrium is reached. The deposition on the lattice, therefore, is nonuniform and noninstantaneous. The radial distribution and the speed of the deposition on the lattice are determined by the electron-phonon coupling, and by the specific heats and thermal conductivities of the electronic and lattice systems.

In our calculations for the thermal spike deposition mode, the initial radial spread of the energy deposited on the electrons is derived from the formulation due to Waligorski.[24] The time development of the deposition is determined by the rate of heat transfer from the electronic to the lattice system and is obtained by numerically solving the heat diffusion equations for the electronic system, and the energy is transferred to the lattice systems.[7,10,15] The deposition on the lattice is implemented as a discrete energy boost or kick to the atoms. The transfer is assumed to stop when the electronic temperature is equal to the lattice temperature; no transfers back from the lattice to the electronic system are permitted. Following Ref. 15, we use a specific heat $C_e=1$ J/K cm^3 and a heat diffusivity $D_e=2$ cm^2/s for the electronic system, independent of space and time. With these assumptions, the length λ over which the heat of the electronic system diffuses depends on the coupling time, which is in turn related to the electron-phonon coupling g.

In this work, we vary λ as a free parameter and the electron-phonon coupling is then calculated from the relation $g=C_e\cdot D_e/\lambda^2$. The initial temperature is assumed to be 0 K. For systems with large energy depositions considered later in this paper, the maximum temperature attained at the boundary is 89 K for cylindrical deposition at an S_e of 100 eV/Å, 94 K for thermal depositions with $\lambda=1$ nm at an S_e of 200 eV/Å, and 100 K for thermal depositions with $\lambda=2$ nm at an S_e of 250 eV/Å. The boundary temperatures were considerably less for the lower values of S_e considered: 18 K for cylindrical deposition with 10 eV/Å, 1 K for thermal depositions with $\lambda=1$ nm at 17 eV/Å, and 1 K for thermal depositions with $\lambda=2$ nm at 20 eV/Å. The simulations are carried out for times ranging from 60 to 100 ps.

III. RESULTS

The variation of sputtering yield with the electronic energy loss S_e for the cylindrical deposition model with a ra-

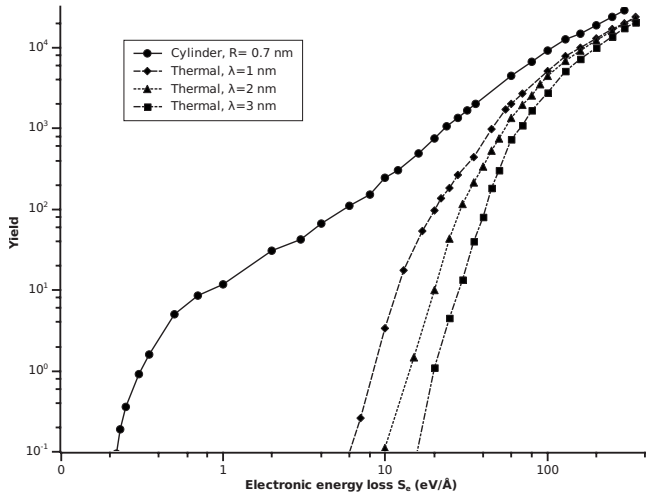

FIG. 1. The sputtering yield plotted as a function of the electronic energy loss.

dius of 7 Å, and thermal spike models with $\lambda=1$, 2, and 3 nm are plotted in Fig. 1. At low S_e, the yield depends dramatically on the model chosen and the parameters; for the same S_e, the yield is more than an order of magnitude higher for cylindrical deposition than for the thermal spike deposition calculations. At high values of S_e, the differences become progressively much smaller.

A direct comparison of the sputtering yield resulting from the two deposition mechanisms in terms of the S_e is not straightforward. Even though the molecular dynamics treatment of sputtering for the two models is otherwise identical, the initial energy of the target atoms before the start of motion and the energy kick imparted to target atoms during the course of the simulation are different for the same S_e. For the cylindrical deposition model, the initial energies are well defined; the S_e values in Fig. 1 represent the total energy deposited equally on all atoms in a cylinder of 7 Å radius at the beginning of the simulation. For the thermal spike deposition, however, the S_e in Fig. 1 represents the total energy deposited initially on the electronic system by the projectile. In this case, the energy deposited on the electronic system is normalized in a way that the integral over time and radius is equal to S_e. The subsequent transfer of energy to the lattice atoms is a continuous process. The atoms gain energy over a period of time, which depends on the coupling parameter. The processes of energy gain, loss to neighboring atoms, and conversion to potential energy continue simultaneously for some time.

The initial energy deposition cannot therefore be separated from the subsequent transport as clearly for thermal spike deposition as is possible for the cylindrical deposition model. An equivalent initial point in time for a spikelike model may be fixed with little ambiguity only in the case that the electronic system loses a major portion of its energy to the lattice before movement of the lattice atoms occurs, and before the atoms start losing significant amounts of energy. Then a time, which may be considered as that of initial deposition, may be determined by finding when the electronic energy has significantly reduced, the kinetic energy of the lattice atoms has peaked, and the cumulative kick imparted to the atoms has saturated.

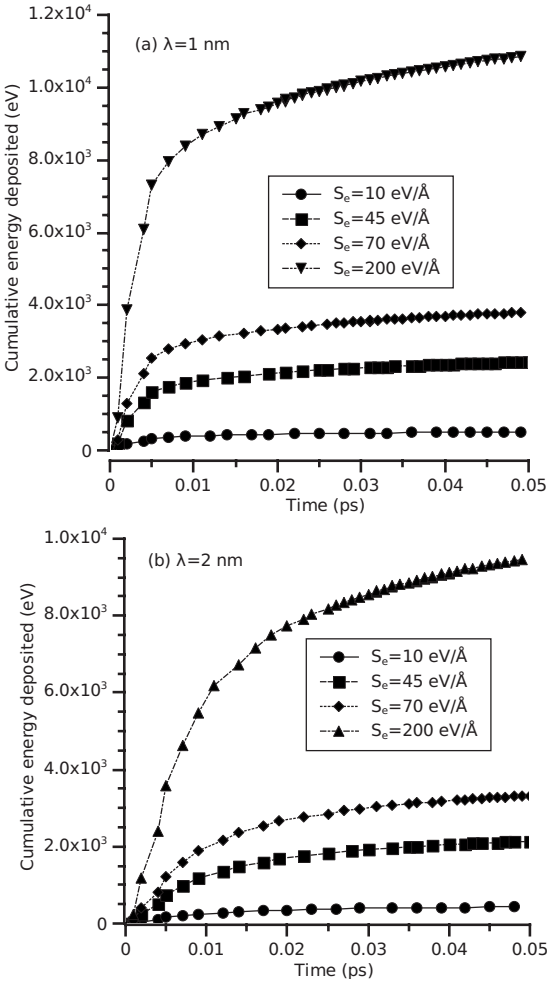

FIG. 2. Time evolution of total energy transferred to lattice atoms for thermal deposition with the energy summed over all atoms receiving kick $E>0.001$ eV: (a) $\lambda=1$ nm and (b) $\lambda=2$ nm.

To check whether such a condition is indeed realized, a cylinder containing the initially energized atoms may be defined, and the time evolution of the kinetic energy and the energy transferred from the electronic system for the atoms in this cylinder may be calculated. Any definition of this initially energized cylinder is necessarily arbitrary. We use two different definitions of the radius to see if it is possible to find a time for which the conditions above are satisfied. The time evolution of the cumulative energy deposited on the lattice, totaled over all atoms that have received an energy kick of at least 0.001 eV, is plotted in Fig. 2. Most of the energy is transferred during the period between 0.007 and 0.05 ps, depending on the S_e. At the largest values of S_e for $\lambda=1$ nm and $\lambda=2$ nm, more than 70% of the total-energy transfer is completed by 0.02 ps. This proportion is more than 90% for lower S_e values. The time evolution of the cumulative transferred energy for atoms in a cylinder of radius $0.7R_0$, where R_0 is the radius of the minimal cylinder that includes the positions at $t=0$ of all finally sputtered atoms, is displayed in Fig. 3. For this definition of the radius, the energy transfer to the atoms stops at times between 0.007 and 0.025 ps. The kinetic energy of the atoms in the cylinder defined like this starts falling off after 0.02 ps (Fig. 4).

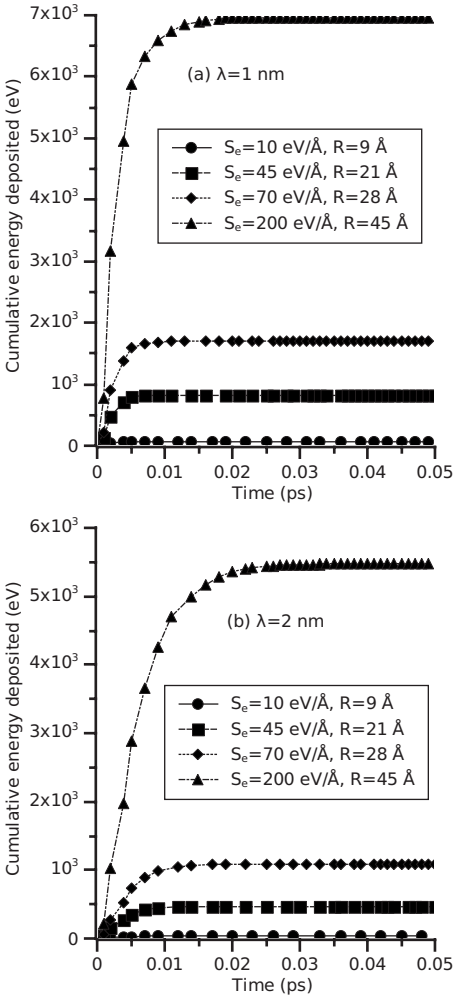

FIG. 3. Time evolution of total energy transferred to lattice atoms for thermal deposition with the energy summed over all atoms in cylinder of radius $R=0.7R_0$, where R_0 is the radius of the minimal cylinder that includes the positions at $t=0$ of all finally sputtered atoms: (a) $\lambda=1$ nm and (b) $\lambda=2$ nm.

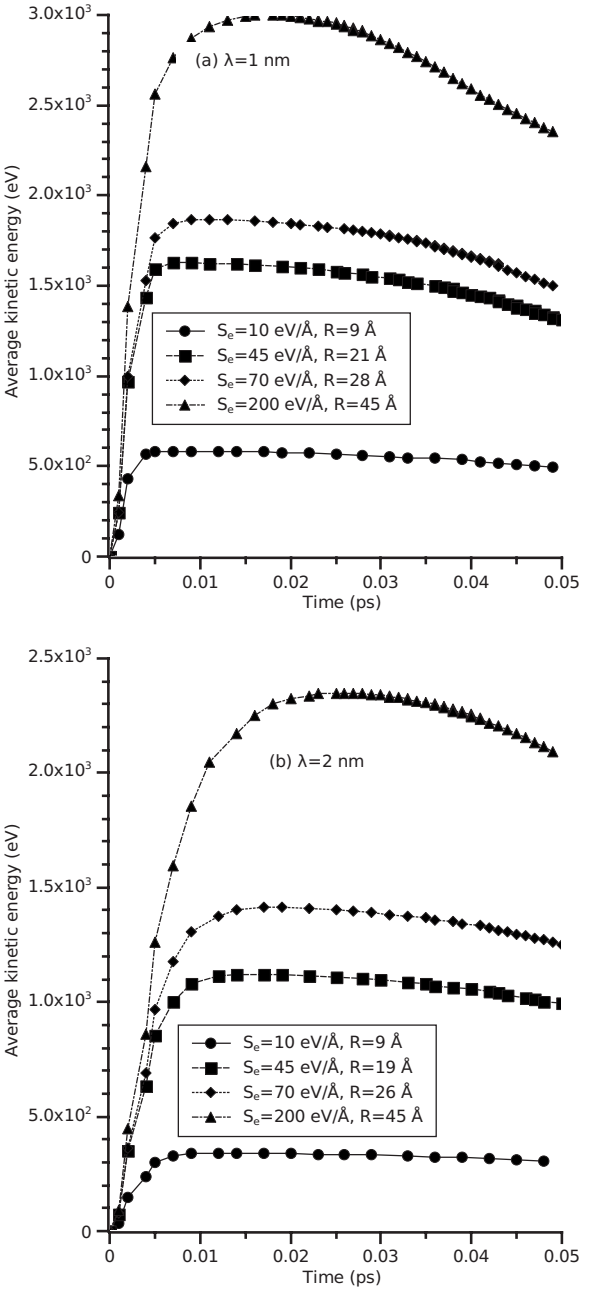

FIG. 4. Time evolution of kinetic energy of lattice atoms summed over all atoms in cylinder of radius $0.7R_0$, where R_0 is defined by positions at $t=0$ of all finally sputtered atoms: thermal deposition with (a) $\lambda=1$ nm and (b) $\lambda=2$ nm.

Independent of the method used to define the initially affected cylinder around the track core, therefore, a window between 0.007 and 0.02 ps may be defined when the atoms have received almost all the energy from the electronic system, and before significant changes to the lattice have occurred. The yield as a function of energy deposition on the atoms at $t=0$ for cylindrical deposition, and $t=0.007$ and 0.02 ps for thermal deposition with $\lambda=1$ nm and $\lambda=2$ nm, is plotted in Fig. 5. The trends are very similar for the earlier and later values of simulation time for the thermal spike depositions. Either one may then be used to extract information on the role of the radial distribution alone on the sputtering yield. We define the energy deposition on all atoms receiving a kick larger than 0.001 eV at $t=0.02$ ps for the spikelike models as the energy deposition on the lattice; this deposition is referred to henceforth as $S_{i,0.001}$, or simply S_i for brevity. This enables a comparison with the initial energy deposition $S_i=S_e$ in the cylinder deposition model.

We note here that, in the analytical thermal spike model, the electron-phonon mean-free time τ can be deduced from the electron-phonon mean-free path by the relation $\lambda^2=D_e\tau$. For $D_e=2$ cm^2/s and $\lambda=2$ nm, $\tau=0.02$ ps, consistent with the above estimate. In our calculations, we see that the subsequent movement of the atoms takes place over tens of picoseconds, and sputtering takes place at times between 10 and 60 ps. These values are in agreement with both thermal spike[10] and fluid dynamics[18] calculations.

The two distinct regimes observed in Fig. 1 persist in Fig. 5. At low initial deposition, the yield for uniform cylindrical deposition is an order of magnitude higher than for the thermal spike deposition for the same S_i. Expectedly, the yield for thermal spike deposition with $\lambda=1$ nm is larger than that

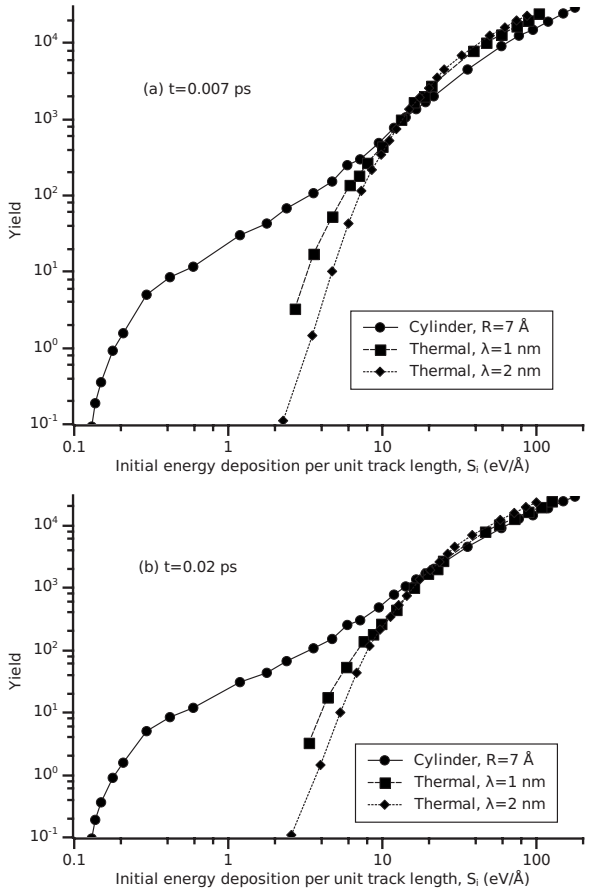

FIG. 5. The sputtering yield plotted as a function of the initial deposited energy with the deposition calculated at (a) simulation time 0.007 ps and at (b) simulation time 0.02 ps for thermal deposition models.

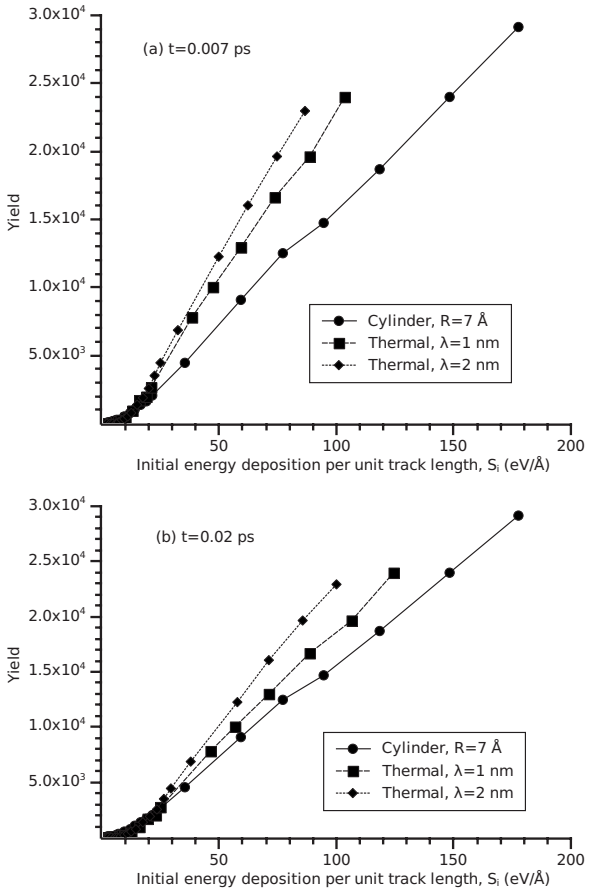

FIG. 6. Same as Fig. 5 but plotted on linear scale to emphasize behavior at high depositions.

for deposition with $\lambda=2$ nm; Due to the lower electron diffusion length and stronger coupling, the deposition with $\lambda=1$ nm is closer to the case of cylindrical deposition than is thermal deposition with $\lambda=2$ nm.

At total initial deposited energies above a few hundred eV, the yield for spikelike models is larger for the same total deposited energy than for the cylindrical deposition model; the plots in Fig. 5 are displayed on a linear scale in Fig. 6 to emphasize the differences at high initial energy deposition.

In the low S_i regime, the steady increase in the sputtering yield with deposited energy for the cylindrical model above a threshold is consistent with earlier simulations of sputtering following uniform deposition in a cylinder of fixed radius. The linear dependence of the yield on total energy deposited above a threshold corresponding to the cohesive energy of 0.08 eV is a feature of both molecular dynamics[12–14] and fluid dynamics[18] calculations. For low total initial energy deposition, the number of atoms with high initial energy is also larger for the cylinder model than for thermal deposition, where the energy is spread over a larger number of atoms. It is conceivable that there is a more efficient contribution to sputtering by atoms that have received a higher initial energy. The yield against total initial deposition $S_{i,0.08}$ calculated for only those atoms that start out with a deposited energy greater than the cohesive energy of 0.08 eV is plotted in Fig. 7. A similar scaling is indeed observed for all models at low $S_{i,0.08}$ values.

This argument does not, however, explain the yield observed for high values of initial deposited energy $S_{i,0.08}$ [Fig. 7(b)]. For the same $S_{i,0.08}$, yield for cylindrical deposition is lower than that for thermal deposition. This is similar to the yield dependence on the initial deposition S_i on all atoms (Fig. 6). The yield as a function of the number of atoms with an initial energy kick above 0.025 eV (the displacement energy for our LJ target is 0.0236 eV), and above 0.08 eV, is plotted in Fig. 8. We note the number of atoms is the same, independent of S_e, for the plots of the cylindrical model in Fig. 8; this implies that for all except the lowest S_e, the deposited energy is enough to kick all atoms in the energized cylinder above the threshold values. For cylindrical deposition, the total number of atoms that can receive energy is constrained to the total number of atoms in the 7 Å energized cylinder and all the deposited energy is distributed equally among a relatively small number of atoms. For thermal deposition, the radius of the energized cylinder is assumed to increase with S_e. This implies more energized atoms for larger S_e. Further, the energy is not distributed equally but falls off with radial distance from the projectile track; consequently, many energized atoms may be expected to receive a relatively small amount of energy. From Fig. 8, it is clear that for all but the smallest values of deposited energy, a larger number of atoms is energized above the

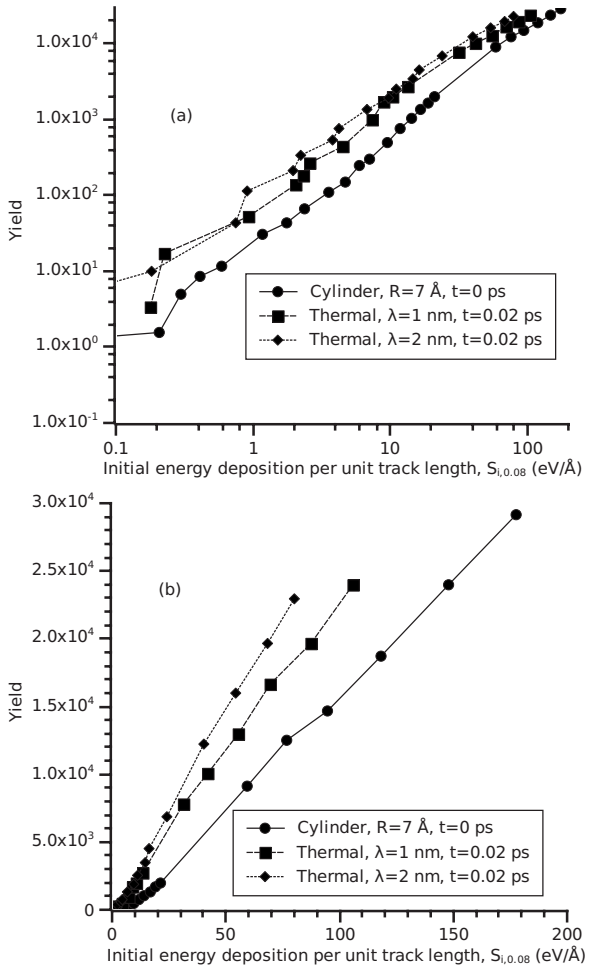

FIG. 7. (a) The sputtering yield plotted as a function of the initial deposited energy of atoms receiving an initial energy kick of more than 0.08 eV. The initial kick for thermal models has been calculated at $t=0.02$ ps. (b) Same as (a) but plotted on a linear scale to emphasize behavior at high energy depositions.

0.025 and 0.08 eV threshold values for the thermal deposition model than for cylindrical deposition at any given value of S_i. It is also apparent that the sputtering yield cannot be related simply to a threshold value for the initial deposition on an atom: for the cylindrical model, the yield rises with S_i even though the number of atoms above the threshold does not change.

The dependence of the yield on the deposited energy appears thus to be amenable to different explanations for low and high S_i. At low S_i values, the dependence is consistent with the assumption that a minimum threshold deposition on an atom is necessary for a contribution to sputtering. This is not the case for large S_i values. Instead, a higher yield is associated with the deposited energy being spread out to a larger number of atoms in a bigger radius (Figs. 5–7). A possible explanation for this may lie in the competition between radial flow and sputtering in the dissipation of the deposited energy.[18,20] In thermal spikelike models, the expansion of the electron gas during the deposition process means that atoms farther away from the projectile track core are directly able to receive energy from the electronic system. Analytical thermal spike calculations show the relation between the expansion of the electron system and the heating of the track core;[23] the heating time determined from these calculations is nearly equal to the mean-free time deduced from the electron-mean-free path. The increase in the temperature near the core track is thus related to the heating time, given by the electron energy expansion. In a cylindrical deposition model, however, radial expansion takes place after the deposition and part of the deposited energy is transferred to atoms outside the initially energized cylinder. For large S_i, most of the sputtering does indeed involve atoms that have not initially been energized; while only a few hundred atoms in a 7 Å cylinder are directly assigned energies at $t=0$, the sputtering yield reaches thousands and the radius R_0 of the minimal cylinder enclosing the positions at $t=0$ of the sputtered atoms reaches tens of angstroms. The lower yields observed for cylindrical deposition in Fig. 7(b) are then indicative of some dissipation of the initial deposited energy in the process of radial expansion and transfer to atoms outside the initially energized cylinder.

The radial distribution of the deposited energy may be quantified for thermal spike deposition by defining a threshold for the energy deposition on a single atom, above which the atom may be considered to be energized. A threshold value of 0.001 eV is low enough to ensure that almost all atoms that have received any energy during the transfer process are counted among the energized. The smallest cylinder enclosing all such energized atoms will be referred to as an energized cylinder. At low initial deposition values, the radius of the energized cylinder for the thermal spike model calculations is greater than but still comparable to the 7 Å radius for the cylindrical deposition model. Above a few hundred eV of total deposited energy, the number of energized atoms (Fig. 9) and the radius of the energized cylinder (Fig. 10) are much larger for thermal spike deposition than for the cylindrical deposition model.

The size of the sputtering yield has been shown to be linked to the transport of energy to the surface.[13] The part of the initial deposited energy that goes into sputtering can thus be expected to be related to the axial kinetic energy of the atoms in the bulk. A comparison of the axial kinetic energies of atoms in the initially energized cylinder and the cylinder enclosing the initial positions of atoms that are finally sputtered is instructive. The time evolution of the total and axial components of kinetic energy summed over all atoms, for small and large S_i, is plotted in Fig. 11. The time evolution of the number of atoms with axial kinetic energy greater than the surface binding energy of 0.08 eV for cylindrical and thermal spike depositions is plotted in Fig. 12, with S_e chosen to provide similar initial energy depositions S_i on the lattice. For smaller energy depositions where the radii of the energized cylinder are similar for all models, the axial kinetic energies are larger for cylindrical deposition than for thermal deposition and larger for the thermal spikelike deposition with $\lambda=1$ nm than for $\lambda=2$ nm. For large energy depositions, this difference is much less significant.

The time evolution of the total and axial kinetic energies summed over all atoms in a cylinder of radius $0.7R_0$ is plotted in Fig. 13. The transfer of energy from atoms in the initially energized cylinder to atoms outside for the cylinder

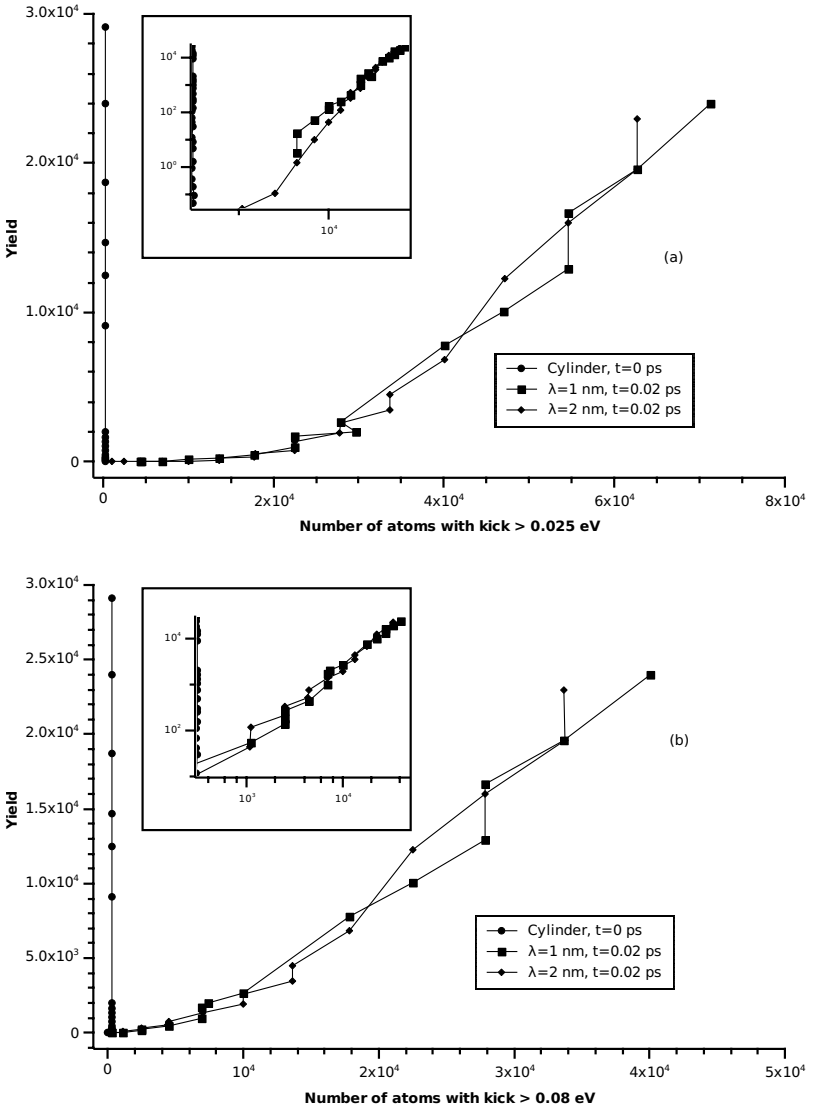

FIG. 8. Yield vs number of energized atoms with initial kick of more than (a) 0.025 and (b) 0.08 eV. The same x values for the cylindrical plots imply that all atoms in the energized 7 Å cylinder have initial energies above threshold values 0.025 and 0.08 eV. The plots are reproduced on a log scale in the insets to emphasize behavior at a small number of energized atoms.

deposition is reflected in the falling off of the 7 Å curve relative to the 41 Å curve. The difference between the energy for the initially energized 7 Å cylinder and the larger 41 Å cylinder is more pronounced for the total than for the axial kinetic energy. While the total kinetic energy is higher for cylinder deposition than thermal deposition for atoms in the $0.7R_0$ cylinder at large S_e, the axial kinetic energy [Fig.

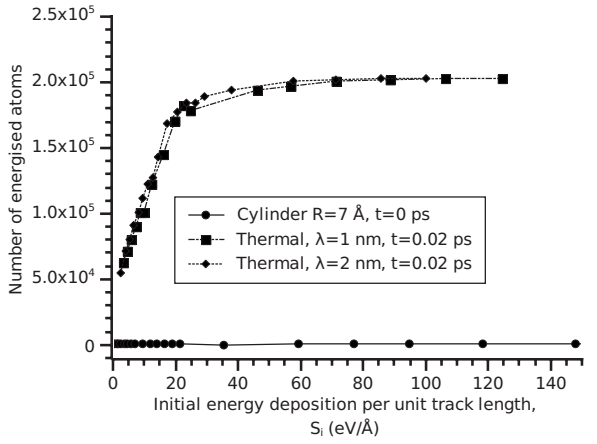

FIG. 9. Number of energized atoms as a function of total initial deposited energy. Atoms are considered to be energized if they receive a cumulative kick $E>0.001$ eV.

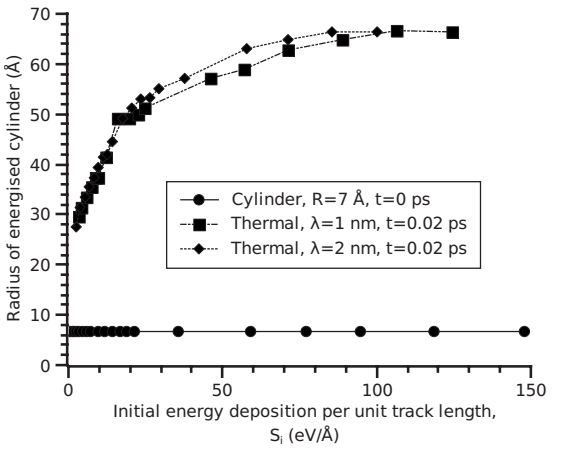

FIG. 10. Radius of energized cylinder as a function of total initial deposited energy.

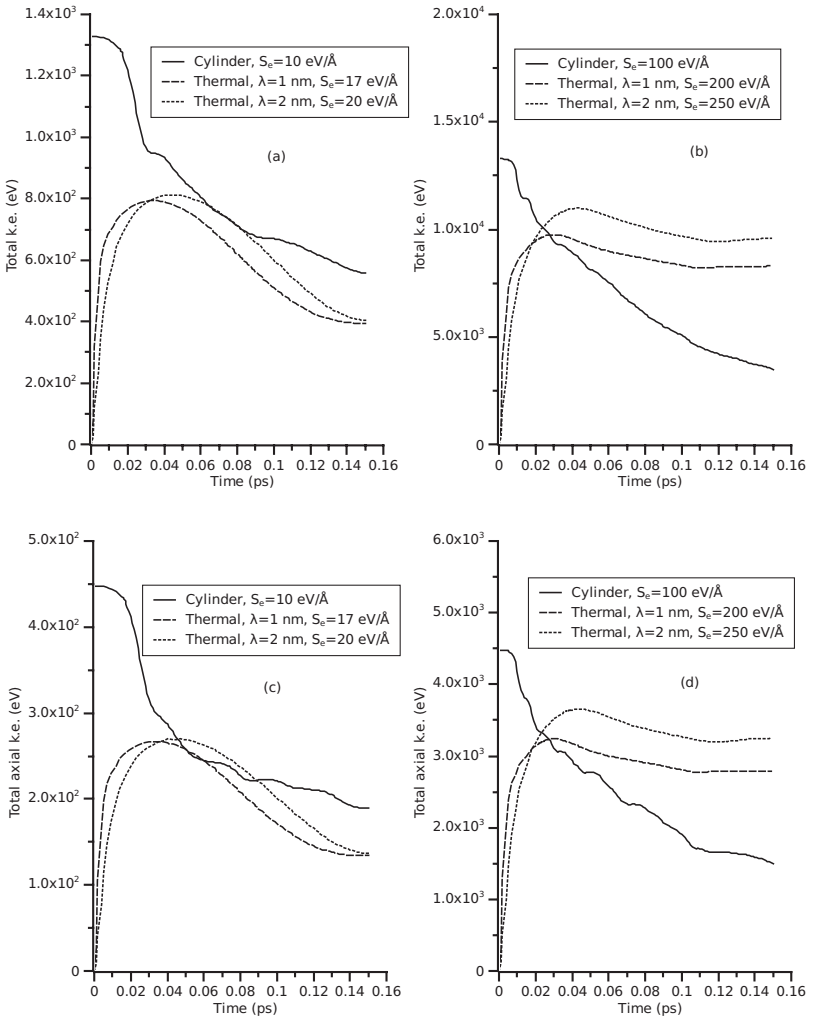

FIG. 11. Time evolution of kinetic energy summed over all atoms with initial kick energy $E > 0.001$ eV. (a) Kinetic energy for small total initial kick. (b) Kinetic energy for large total initial kick. (c) Axial component of kinetic energy for small total initial kick. (d) Axial component for large total initial kick. S_e values chosen to compare similar values of initial total kick to atoms.

13(d)] is comparable for the two deposition mechanisms. This is reflected in the plots in Fig. 12 as well: the number of atoms with an axial kinetic energy greater than 0.08 eV is much larger for cylinder deposition at low S_i and much smaller than for thermal deposition at large S_i. The overall trend is similar to that in Fig. 11; the axial kinetic energy is larger for cylinder deposition at low S_i and not very different from thermal spike deposition at high S_i. This is consistent with the trends for the yield at low and high values of the total deposited energy. We may conclude from this that for cylinder deposition at high S_i values, the energy transfer out of the initially energized cylinder appears to result in a less than proportional increase in the axial kinetic energy of atoms outside. For low S_i, however, this does not appear to be a factor, and atoms receiving energy above a threshold contribute efficiently to sputtering for both cylindrical and thermal spike depositions.

IV. CONCLUSIONS

Using different values of the electron-lattice coupling for the femtosecond- scale deposition of energy from the electronic system to the lattice, and the same classical molecular dynamics framework for atomic motion and sputtering from

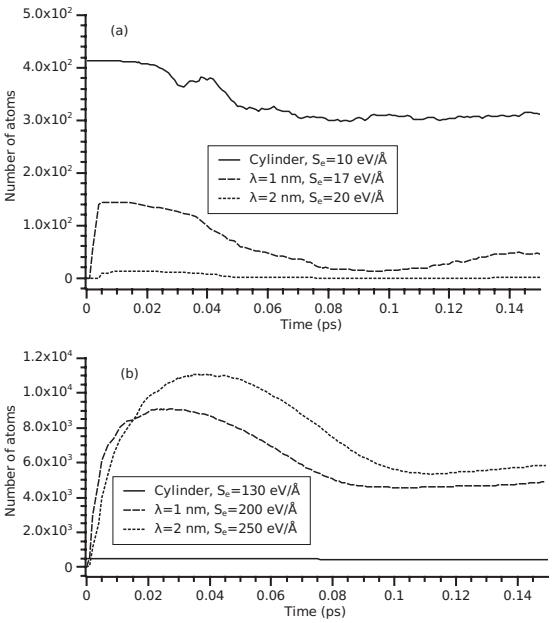

FIG. 12. Time evolution of the number of all atoms with axial kinetic energy above the surface binding energy for small and large energy depositions. S_e values chosen to compare similar values of total-energy kick to atoms.

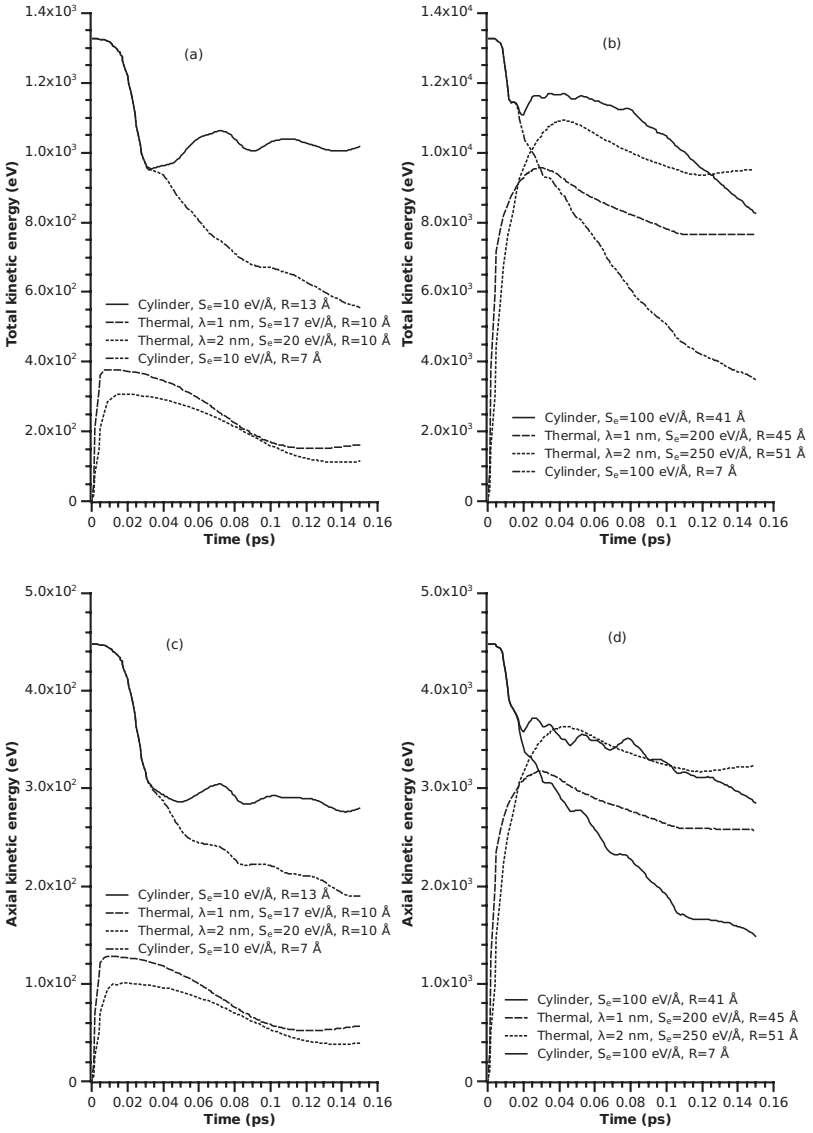

FIG. 13. Time evolution of kinetic energy summed over all atoms in cylinder of radius $0.7R_0$. (a) Kinetic energy for small total initial kick. (b) Kinetic energy for large total initial kick. (c) Axial component of kinetic energy for small total initial kick. (d) Axial component for large total initial kick. S_e values chosen to compare similar values of initial total kick to atoms. The plot for cylinder deposition with R=7 Å (Fig. 11) is included for comparison.

a Lennard-Jones target, we observe a strong influence of the radial distribution of the initially deposited energy on the sputtering yield. The yield dependence reflects the radial expansion, in the thermal spikelike models, of the electronic system prior to the transfer of energy to the lattice. While the sensitivity of the yield to the time and radial distributions of the initial energy deposition offers the possibility of a more precise understanding of the electron-lattice coupling, it also points to the need for more complete modeling of the transfer process in order to facilitate comparisons with experiment.

ACKNOWLEDGMENTS

The authors are grateful to H. M. Urbassek for the use of the IMPACT code.

*sumit@iuac.res.in

[1] M. Skupinski, M. Toulemonde, M. Lindeberg, and K. Hjort, Nucl. Instrum. Methods Phys. Res. B **240**, 681 (2005).

[2] F. Studer, M. Hervieu, J. M. Costantini, and M. Toulemonde, Nucl. Instrum. Methods Phys. Res. B **122**, 449 (1997).

[3] N. Chtanko, M. E. Toimil-Morales, T. W. Cornelius, D. Dobrev, and R. Neumann, Nucl. Instrum. Methods Phys. Res. B **236**, 103 (2005).

[4] U. Amaldi and G. Kraft, J. Radiat. Res. (Tokyo) **48**, A27 (2007).

[5] J. F. Ziegler, Nucl. Instrum. Methods Phys. Res. B **219-220**, 1027 (2004).

[6] P. Sigmund and A. Schinner, Nucl. Instrum. Methods Phys. Res. B **195**, 64 (2002).

[7] A. Meftah, J. Costantini, N. Khalfaoui, S. Boudjadar, J. P. Stoquert, F. Studer, and M. Toulemonde, Nucl. Instrum. Methods Phys. Res. B **237**, 563 (2005).

[8] M. Toulemonde, W. Assman, C. Dufour, A. Meftah, F. Studer, and C. Trautmann, Mat. Fys. Medd. K. Dan. Vidensk. Selsk. **52**, 263 (2006).
[9] M. Toulemonde, W. Assmann, C. Trautmann, and F. Gruner, Phys. Rev. Lett. **88**, 057602 (2002).
[10] M. Toulemonde, W. Assman, C. Trautmann, F. Gruner, H. D. Mieskes, H. Kucal, and Z. G. Wang, Nucl. Instrum. Methods Phys. Res. B **212**, 346 (2003).
[11] W. Assmann, M. Toulemonde, and C. Trautmann, Top. Appl. Phys. **110**, 401 (2007).
[12] H. M. Urbassek, H. Kafemann, and R. E. Johnson, Phys. Rev. B **49**, 786 (1994).
[13] E. M. Bringa, R. E. Johnson, and L. Dutkiewitz, Nucl. Instrum. Methods Phys. Res. B **152**, 267 (1999).
[14] E. M. Bringa, R. E. Johnson, and M. Jakas, Phys. Rev. B **60**, 15107 (1999).
[15] M. Beuve, N. Stolterfoht, M. Toulemonde, C. Trautmann, and H. M. Urbassek, Phys. Rev. B **68**, 125423 (2003).
[16] D. Schwen and E. M. Bringa, Nucl. Instrum. Methods Phys. Res. B **256**, 187 (2007).
[17] M. M. Jakas and E. M. Bringa, Phys. Rev. B **62**, 824 (2000).
[18] M. M. Jakas, E. M. Bringa, and R. E. Johnson, Phys. Rev. B **65**, 165425 (2002).
[19] E. M. Bringa, M. Jakas, and R. E. Johnson, Nucl. Instrum. Methods Phys. Res. B **164-165**, 762 (2000).
[20] E. M. Bringa and R. E. Johnson, Nucl. Instrum. Methods Phys. Res. B **143**, 513 (1998).
[21] E. M. Bringa and R. E. Johnson, Nucl. Instrum. Methods Phys. Res. B **180**, 99 (2001).
[22] E. M. Bringa, R. E. Johnson, and R. M. Papaleo, Phys. Rev. B **65**, 094113 (2002).
[23] M. Toulemonde, C. Dufour, A. Meftah, and E. Paumier, Nucl. Instrum. Methods Phys. Res. B **166-167**, 903 (2000).
[24] M. P. R. Waligorski, R. N. Hamm, and R. Katz, Nucl. Tracks Radiat. Meas. **11**, 309 (1986).